Translucency Material Analysis by Inverse Rendering and Dipole Approximation

Evelyn Lissete Paiz[1]*

Abstract

Background and Objectives Translucency can be found all around us (e.g. milk, skin, clouds, paint, coffee, etc.). Nevertheless, modeling the interaction of light with these materials is difficult. For this reason, various methods have been proposed to simplify its representation by restricting or approximating the model. Thus, with a viable representation of light interaction, different physical properties of the material can be acquired in practice. Here it is explored the experimental method proposed by Jensen et al. [18] on a dipole BSSRDF model.

Study Design/Materials and Methods The methodology is based on inverse rendering. The basic flow is: (1) illuminate the sample, (2) observe the diffusion of the light, (3) capture and reconstruct the intensity, (4) examine the intensity and (5) fit the data to the model. Since Alkaoui [1] (using a whole milk sample) had already performed the steps one, two and partially three (acquisition of 46 images), only the processing and analysis was carried out (steps three to five).

Results A complete high dynamic range (HDR) image was generated from the dataset of images. To display the result correctly, a global log tone mapping was applied. It was selected a 2D region on the image, where the diffusion of light on the surface was observed on the sample. The slice was averaged to a 1D representation. The algorithm of Debevec and Malik [6] was used to observe the intensity and this result was fitted to the dipole model. From the fitting, it was obtained the absorption σ_a and scattering σ_s' parameters of the sample.

Conclusion It was possible to test a known approximation method (dipole BSSRDF model) on a practical environment and continue the work presented by Alkaoui [1]. The possible improvements for future work are the following: (1) Start the process from the beginning and perform the acquisition again with a sample and a perfect diffuser. (2) Consider testing different samples (e.g. different types of milk - whole , skim, almond, soya, etc.) to see the difference on physical properties for each one. (3) On the final evaluation step, not only measure robustness, but also perform the evaluation based on other existing methods (e.g. photo mapping or Monte Carlo).

Keywords
Translucency — Light Interaction — Dipole BSSRDF Model — Inverse Rendering

[1] *Norwegian University of Science and Technology, Gjøvik, Norway*
***Corresponding author**: elreyes@stud.ntnu.no

Contents

Introduction

Objects that compose people's daily interactions vary on how light is transmitted through them [9]. Translucency is a common visual phenomenon and occurs whenever light penetrates a material and scatters within it before re-emerging towards the observer. This internal scattering can create a variety of image effects, depending on the object's shape and material, its distance from the observer and the composition of the light around it [14]. The degree of translucency may vary, but the appearance is distinctly smooth and soft as a result of the light scattering inside the object. This process is known as subsurface scattering [17].

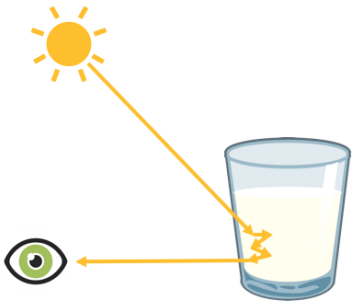

Figure 1. Subsurface scattering example on a translucent material (milk).

How does subsurface scattering works? It diffuses the scattered light and blurs the effect of small geometric details on the surface, softening the overall look of the object. Thus, this scattered light can also pass through the object (particularly noticeable when other objects are seen from behind the material) [17]. This phenomenon contain useful material information and depends on two important physical properties of the object, known as absorption and scattering parameters.

Translucent materials are found all around us (i.e. milk, leaves, skin, paper, clouds, paint, coffee, marble, etc.). Accurately describing and understanding the interaction of light with these materials is one key to understand our world [9]. Currently, computer graphics has been the lead field of research for this phenomenon. However, the interaction of light with these materials also concerns other fields of research (e.g. color science, physics, medicine, etc.), since it affects the human perception of the object. *What does this means?*, it means that humans are capable of discriminate subtle differences in materials and make inferences about physical properties on objects just based on the appearance of the object [14].

Recently researchers are pursuing the goal of predict accurately the physical quantities from a real scene [22], based on the concept of light transport. This notion describes the behavior of light as it is emitted from a light source, interacts with the scene and ultimately arrives to a sensor. Unfortunately, the physical behavior of light is complex and not completely understood, needing simplifying assumptions to allow an efficient modeling [3].

The present work has as main objective to reproduce and evaluate the experimental method proposed by Jensen et al. [18]. Its basis is focused on a simplification of the subsurface scattering for translucent materials using a dipole model. However, here the objective is to use the technique of inverse rendering (see section 3.1) to obtain the two physical properties of translucent materials (absorption σ_a and scattering σ_s' parameters) using the simplify version of Jensen et al. [18]. The main contributions of this work are the following:

1. Evaluation and reproduction of the known approximation dipole method of light transport for translucent homogeneous objects proposed by Jensen et al. [18].
2. Continuation of the work presented by Alkaoui [1], which have already acquired a set of data based on the same translucency principle.
3. Definition and implementation of an inverse rendering approach to determine the physical properties (absorption and scattering parameters) of whole milk.

The rest of this paper is organized as follows. Previous works are discussed in section 1. Section 2 depicts a theoretical background. The methodology is described in section 3 and section 4 explains the proposed experiments with its results. The experimental evaluations are presented in section 5. Section 6 gives the conclusion with a future work remarks.

1. Related Works

Generally, the subsurface scattering has been approximated as a Lambertian diffuse reflection [17]. However, over the years new methods have emerge to improve this approximation. Currently, there is a great amount of research on modeling, rendering, and measuring subsurface scattering. In this section a brief review of state of the art is given in four basic groups: (1) Monte Carlo methods, (2) diffusion methods, (3) similarity theory, and (4) inverse rendering [29].

1.1 Monte Carlo

The Monte Carlo methods solve the subsurface scattering model directly. The work of Kajiya and Von Herzen [19], Lafortune and Willems [20], Pauly et al. [25] (on volumetric path tracing and its variations) provided an unbiased estimators for the solution radiance. This was accomplished by

randomly constructing light paths and evaluating their contributions. Additionally, other techniques such as volumetric photon mapping from Hachisuka et al. [16] and many-lights method from Dachsbacher et al. [4], have been developed. These ones offer faster convergence than path tracing methods, but often at the cost of introducing bias in the results.

1.2 Diffusion

The diffusion methods replace the subsurface scattering model by applying a first order approximation to directional radiance. Several approaches have been proposed to solve it. One is the analytical solution approximation, which includes the work of Jensen et al. [18], D'Eon and Irving [7]. On the other hand, also exists a finite element (or finite difference) based methods, which covers the contributions of Stam [26], Wang et al. [27], Arbree et al. [2].

Nevertheless, a diffusion approximation requires a resulting smooth radiance field. This condition is usually violated near the boundaries of the material and also in the thin regions. Therefore, hybrid methods that combines Monte Carlo (from section 1.1) and the diffusion approximation have been developed to obtain a better accuracy (Li et al. [21], Donner and Jensen [10], Habel et al. [15]).

1.3 Similarity Theory

The similarity theory was introduced by Wyman et al. [28]. Its basis is a derivation of a set of relations between two sets of scattering parameters, so that the resulting subsurface model has identical solution radiance fields when the directional frequencies are bounded. The method has been applied only in a highly simplified order one form. However, very limited work has been done on computer graphics and applied physics, to utilize such relations at higher orders.

1.4 Inverse Rendering

The inverse rendering methods solve for the material properties in a scene given the desired appearance. These techniques have many applications in appearance acquisition. It exists different methods that have been developed to recover subsurface scattering properties proposed by Wang et al. [27], Dobashi et al. [8], Papas et al. [24], Gkioulekas et al. [13].

2. Background

In this section, only the basic concepts of a theoretical background (for the understanding of further sections) is described. For a complete explanation of the mathematical theory, please refer to the work of Jensen et al. [18], Donner [9], Bitterli [3]. Additionally, figure 2 shows the description of the used symbols.

$\vec{x}_i$	Surface location of incident light
$\vec{\omega}_i$	Incident direction
$\vec{x}_o$	Surface location of exitant light
$\vec{\omega}_o$	Exitant direction
$\vec{n}$	Surface normal
f_r	BRDF
f_t	BTDF
S	BSSRDF
$S^{(0)}$	Reduced radiance
$S^{(1)}$	Single scattered radiance
S_d	Multiple scattered radiance
L	Radiance
L_r	Reflected radiance
L_i	Incident radiance
E_i	Irradiance
Φ_i	Incident flux
D	Diffusion constant
ϕ	Fluence
$\vec{E}$	Flux
p	Phase function
g	Mean cosine of scattering angle
σ_a	Absorption coefficient
σ_s	Scattering coefficient
σ'_s	Reduced scattering coefficient: $(1-g)\sigma_s$
σ_t	Extinction coefficient: $\sigma_s + \sigma_a$
σ'_t	Reduced extinction coefficient: $\sigma'_s + \sigma_a$
α	Albedo: σ_s/σ_t
α'	Reduced albedo: σ'_s/σ_t
σ_{tr}	Effective transport coefficient: $\sqrt{\sigma_a/D}$
Q	Source function
η	Relative index of refraction
F_r	Fresnel reflectance
F_t	Fresnel transmittance
F_{dr}	Average Fresnel reflectance
l	Mean free path (mfp): $1/\sigma_t$
l'	Reduced mean free path: $1/\sigma'_t$
l_d	Diffuse mean free path (dmfp): $1/\sigma_{tr}$
R_d	Diffuse reflectance

Figure 2. Symbols used for mathematical representations.

How is light transported beneath the surface of translucent materials?

A geometric optics model is capable of describing the majority of light interactions. This model is based on the assumption that light propagates along straight lines (rays), with infinite speed. The radiance along a ray is considered to be constant and the medium through which the ray travels does not influence on the light transport. These light rays are only capable of change direction at a discrete set of scattering locations, at which their respective energies may be partially absorbed and the remaining fraction scattered into new directions [3].

For most applications, an acceptable approximation is to restrict the location of scattering events to only the surface of the objects. In this model, rays of light travel without scattering until they strike the surface of an object, at which point they are either absorbed completely or scatter and leave the

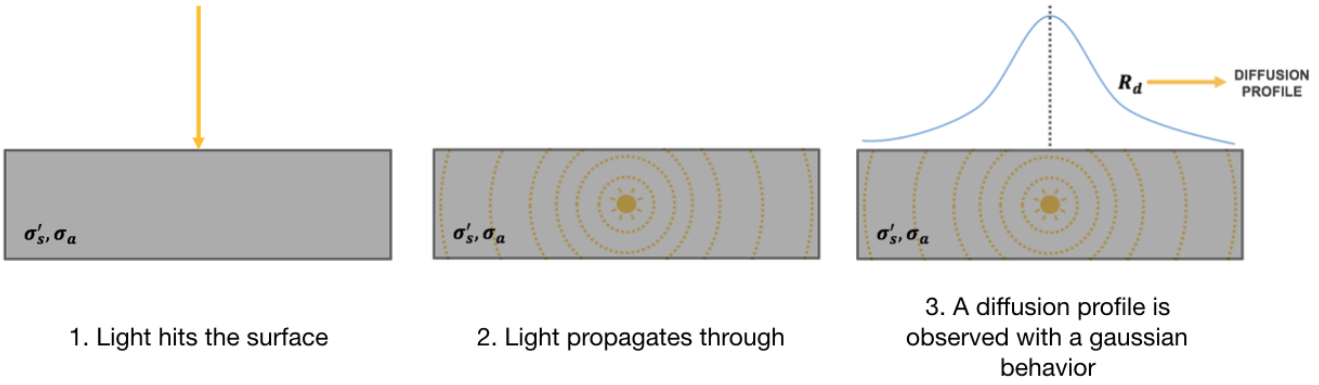

Figure 3. The searchlight problem.

surface at the same location in new directions. This notion is known as the bidirectional reflectance distribution function (BRDF) introduced by Nicodemus et al. [23]. The principle of the model consists on a ray coming from direction ω_i and predicts that the ray strikes a surface at location x and leaves at the exact point x in direction $\vec{\omega}_o$ [3] (see figure 4).

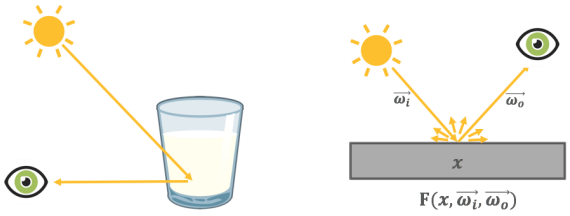

(a) BRDF (bidirectional reflectance distribution function).

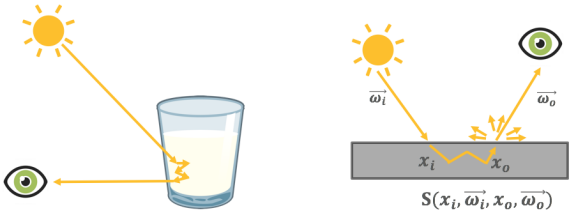

(b) BSSRDF (bidirectional scattering surface reflectance distribution function).

Figure 4. Two known models to represent scattering of light.

However, BRDF is not enough to model correctly all materials. Light scattering in translucent materials is described correctly by the bidirectional scattering surface reflectance distribution function (BSSRDF, also proposed by Nicodemus et al. [23]). The BSSRDF (represented by the function S), defines the general transport of light between two points and directions as the ratio of the radiance $L_o(x_o, \vec{\omega}_o)$ exiting at position x_o in direction $\vec{\omega}_o$ to the radiant flux $\Phi_i(x_i, \vec{\omega_i})$ incident at x_i from direction $\vec{\omega}_i$ (figure 4b) [11] . Therefore, BRDF is actually a special case of BSSRDF where $x_o = x_i$.

$$dL_o(x_o, \vec{\omega}_o) = S(x_i, \vec{\omega}_i; x_o, \vec{\omega}_o) d\Phi_i(x_i, \vec{\omega}_i)$$
$$L_o(x_o, \vec{\omega}_o) = \int_A \int_{2\pi} S(x_i, \vec{\omega}_i; x_o, \vec{\omega}_o) L_i(x_i, \vec{\omega}_i)(\vec{n} \cdot \vec{\omega}_i) d\omega_i dA(x_i) \tag{1}$$

From equation 1, can be noticed that it is necessary to integrate the product of the BSSRDF and the incident radiance for all incident directions and surface locations. This makes evaluation really complex and numerically expensive. A problem setting known as "the searchlight problem" (figure 3) considers a focus of infinitesimally thin pencil beam in the material surface at normal incident. The photons originating in the beam travel along the refracted ray until they are scattered by the medium, leading to a series of scattering events until they are ultimately absorbed or escape through the surface. These distribution of photons exiting through the surface gives rise to a radially symmetric reflectance distribution profile represented as $R_d(\vec{x})$ [3].

Despite that normally the S function from the BSSRDF model cannot be constructed exactly from R_d, many methods approximate S using the reflectance distribution profile R_d. The diffusion approximation introduced by Stam [26] has been used to approximate multiple scattering using this idea. Building on this work, Jensen et al. [18] introduced a practical diffusion dipole model. The model works on three key aspects that make it possible: (1) principle of similarity, (2) a diffusion approximation and (3) the dipole approximation.

2.1 Principle of Similarity

The principle of similarity approximates highly scattering, directional medium by an isotropic medium with modified "reduced" coefficients. This is based on the observation that in highly scattering media, the distribution of light loses dependency from the angle and tends to be isotropy.

2.2 Diffusion Approximation

One of the most successful method for approximating the diffuse reflectance profile R_d is the diffusion approximation. It only considers the angular integrals (n moments) of the radiance. To arrive to the approximation, the radiance is first expanded in spherical harmonics. This expansion is then truncated at the first order and renormalized to conserve energy. This gives an approximation of the radiance in terms of fluence ϕ and flux $\vec{E}$. The result is added to the radiative transport equation and integrated over all directions. Equation 2 show the result approximation for both fluence and distribution profile [3], where $\vec{E}(x) = -D\nabla\phi(x)$, $D = \frac{1}{3\sigma_t'}$ and $r = ||x_o - x_i||$.

$$
\begin{aligned}
R_d(r) &= -D\frac{\vec{n}\cdot\vec{\nabla}\phi(x_o)}{d\Phi_i(x_i)} \\
\phi(x) &= \frac{\Phi}{4\pi D}\frac{e^{-\sigma_{tr}r(x)}}{r(x)}
\end{aligned}
\tag{2}
$$

2.3 Dipole Approximation

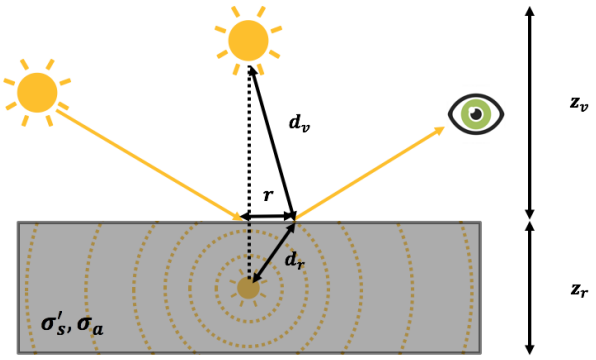

Figure 5. Dipole approximation.

Several methods for solving diffusion boundary conditions are available. However, the dipole approximation states that the closed-form solution of diffusion can be obtained by placing two virtual point sources (in and outside of the medium), as seen in figure 5. By substituting this conditions on equation 2, the close form solutions of both fluence and distribution profile can be found (equation 3).

$$
\begin{aligned}
\phi(x) &= \frac{1}{4\pi D}\left(\frac{e^{-\sigma_{tr}d_r}}{d_r} - \frac{e^{-\sigma_{tr}d_v}}{d_v}\right) \\
R_d(r) &= \frac{\alpha'}{4\pi}\left[(\sigma_{tr}d_r + 1)\frac{e^{-\sigma_{tr}d_r}}{\sigma_t' d_r^3} + z_v(\sigma_{tr}d_v + 1)\frac{e^{-\sigma_{tr}d_v}}{\sigma_t' d_r^3}\right]
\end{aligned}
\tag{3}
$$

3. Materials and Methods

The main goal of the study is to reproduce the experimental method proposed by Jensen et al. [18] (based on the dipole BSSRDF model) on different translucent materials. In this case, to determine the physical properties (absorption σ_a and scattering σ_s' parameters) of whole milk. The method is based on a technique best known as inverse rendering and was used along with the High Dynamic Range (HDR) method proposed by Debevec and Malik [6]. Additionally, was used the dataset already acquired by Alkaoui [1] on her Master Thesis.

3.1 Inverse Rendering

Rendering can be defined as the process of forming an image from a specific scene. However, the technique in which it is acquired the scene information from an image is known as inverse rendering [22]. Based on this concept and the method described by Jensen et al. [18], an inverse rendering methodology towards BSSRDF is used (figure 7). The objective is to acquire the information of the physical properties that are contained in the the material present in the scene.

The method can be divided in two main workflows: (1) an acquisition and (2) the processing plus analysis of the acquired data. Is important to notice that the following work only focuses on the processing and analysis part. For the acquisition, the already captured dataset of images from Alkaoui [1] was used (see section 3.3 for details).

3.1.1 Acquisition

The acquisition process follows the dipole model from Jensen et al. [18]. Therefore, the experimental setup for this process is the one describe in figure 6. The acquisition is divided in three steps: (1) illumination, (2) diffusion and (3) intensity capture.

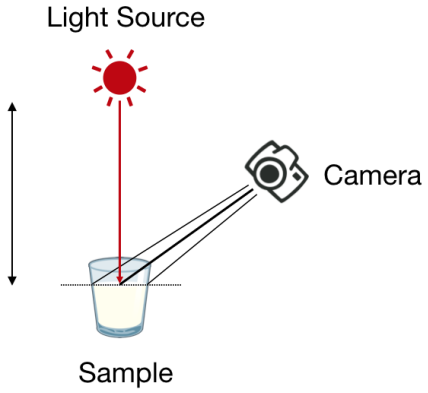

Figure 6. Setup for inverse rendering described by Jensen et al. [18].

1. **Illumination:** The sample (in this case, a glass full with whole milk) is illuminated with a fixed amount of

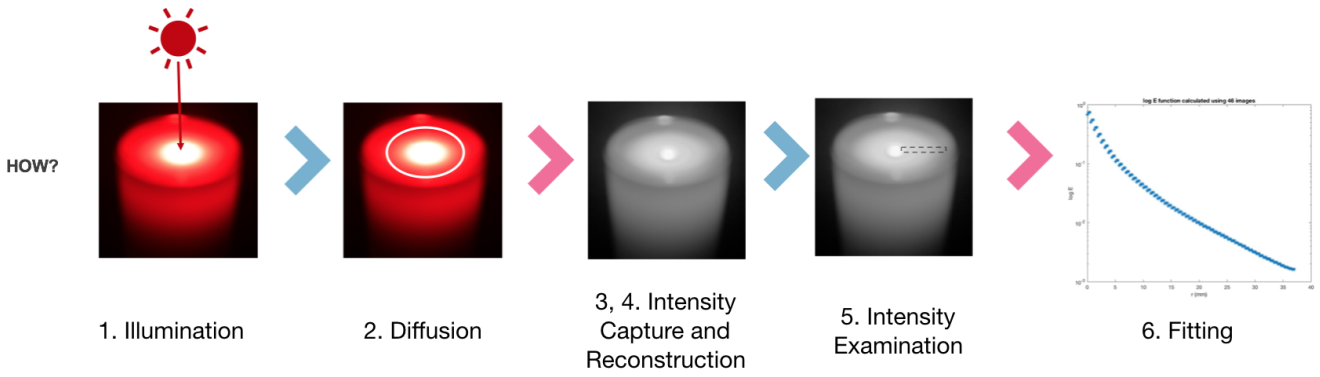

Figure 7. Methodology used for an inverse rendering described by Jensen et al. [18].

light.

2. **Diffusion:** The light diffuses through the material and spreads out in a large area.

3. **Intensity capture:** The intensity of the reflected light is captured by a camera using a High Dynamic Range (HDR) method (a set of images with different exposure times are acquired).

3.1.2 Processing and Analysis

From the data captured in the acquisition process (images with different exposure times), the processing and analysis performed. The procedure is divided in three steps: (1) intensity reconstruction, (2) intensity examination and (3) fitting of the data to the dipole model.

1. **Reconstruction:** The HDR photograph with the intensity information is reconstructed from the captured images with different exposure times.

2. **Intensity examination:** It is examined a slice of the image to see the intensity change through it. Applying the Debevec and Malik [6] method, the result is a radiance map, where the radiant exitance is equal to the pixel values of the slice. A falloff of the intensity will be observed.

3. **Fitting:** The physical properties of the material (absorption and scattering parameters) are estimated by fitting the model described in equation 3 to the reflectance profile from the previous step.

3.2 Radiance Map from Photographs

The high dynamic photographic technique was introduced by Debevec and Malik [6]. It allows an accurate measurement of a scene radiance from a set of differently exposed photographs. Such series of photographs can be combined into a single high dynamic range image called a radiance map. The method allows both low levels of indirect radiance from surfaces and high levels of direct radiance from light sources to be recorded [5].

How is this done?, the observed pixel value $Z_{i,j}$ for pixel i in the image j, is a function of unknown scene radiance and known exposure duration:

$$Z_{i,j} = f(E_i \, \Delta t_j)$$

E_i is the unknown scene radiance at pixel i, and scene radiance integrated over some time $E_i \, \Delta t_j$ is the exposure at a given pixel. In general, f is a complicated pixel response curve. Therefore, the aim is to not solve for f, but for $g = ln(f^{-1})$, which maps from pixel values (0 to 255) to the *log* of exposure values:

$$g(Z_{i,j}) = ln(E_i) + ln(t_j)$$

.

Consequently, after solving g it is straightforward to map from the observed pixels values and exposure times the radiance E_i [12]. Please refer to Debevec and Malik [6] work for the full explanation of the process (specially sections 2.1 and 2.2). Here, it is used their provided algorithm to compute both g and E_i.

3.3 Dataset Definition

Alkaoui [1] worked her Master Thesis on the topic of *Translucent Material Analysis and Modeling*, where she acquired a set of images using the acquisition process from section 3.1.1. The materials used for the setup (figure 6) were the following:

- **Light source:** A monochromatic light source represented as a red laser.
- **Camera:** Nikon D3100 with a tripod for support.
- **Sample:** As a translucent material it was used whole milk.

A thin beam of red light was sent on the surface of the milk and a range of picture were taken varying just the exposure time. The result was a dataset of 46 images with values of exposure times from $\frac{1}{4000}$ up to 8 seconds. Figure 8 shows a sample of the dataset.

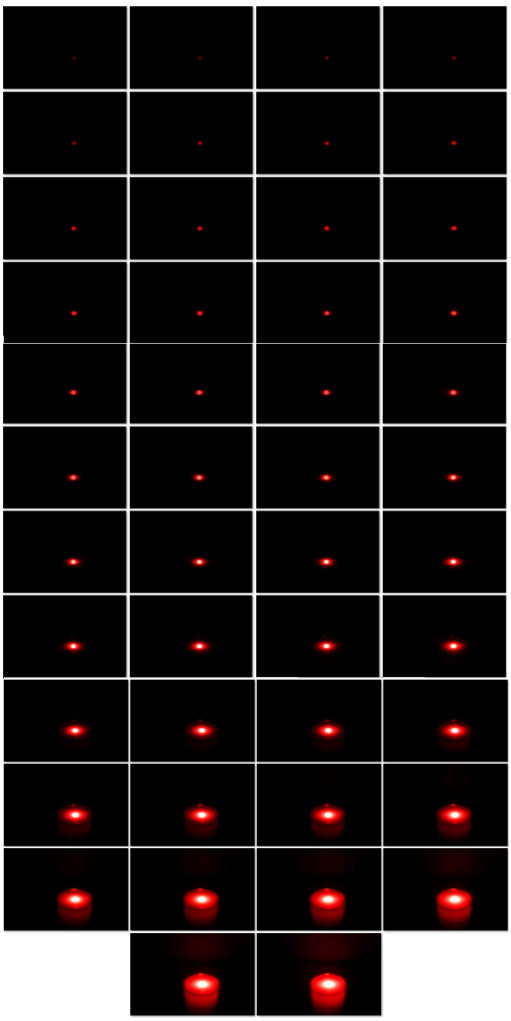

Figure 8. Images captured by Alkaoui [1] for her Master Thesis based on the acquisition process of inverse rendering.

4. Experiments and Results

Four main experiments were performed to implement correctly the processing and analysis of the inverse rendering method (section 3.1.2). The experiments were the following: (1) reconstruction of the HDR image, (2) intensity examination, (3) data fitting and (4) evaluation. In this section a description of the experiments is given along with their results. Note that all the computation was done using Matlab as the working programing language and only the red channel from the images was used (since the source of light was a red laser).

4.1 Reconstruction of the HDR Image

The reconstruction process began with the dataset described on section 3.3. The photographs (representing a set of low dynamic range (LDR) images) and their exposure times were combined to generate the high dynamic range (HDR) image. Getting this final HDR image was only half of the process. The next step was to show the image with its corresponding intensity. Therefore, a tone mapping method was necessary to be applied on the image. The global tone mapping operator $log(L)$ was used. Figure 9 shows the final displayed result.

Figure 9. Resulting HDR photograph applying a log tone mapping.

4.2 Intensity Examination

From the displayed tone mapped HDR image, it was possible to select a representing area where the diffusion of the light was visible on the sample (discarding the laser point and the glass). Therefore, a 2D area of interest from the HDR image was selected manually and from it the other 46 LDR images were crop.

Because the objective was to evaluate just a 1D slice instead of 2D, an average image for each 2D cropped image was obtained. To this set of 1D slice images, the Debevec and Malik [6] algorithm was applied and the g and $log(E)$ curves were obtained. Each curve presented the following:

$g(z)$ was the log exposure corresponding to pixel value z.

$log(E(i))$ was the log film irradiance at pixel location i.

The 2D area of interest selected and the resulting curves of g and $log(E)$, are showed on figure 10.

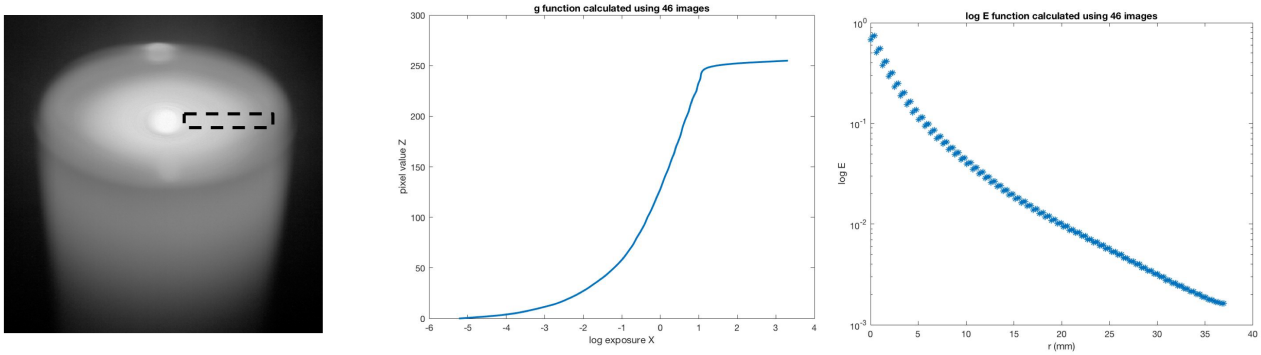

(a) Slice selection.

(b) g function.

(c) $log(E)$ function.

Figure 10. Intensity evaluation only on a selected slice of the images.

4.3 Data Fitting

The first step was to develop a correct representation of the R_d function (equation 3), based only on r and the absorption σ_a and scattering σ_s' parameters:

```
%% ------------------------------------------------
% Norwegian University of Science and Technology
% Evelyn Paiz
% Specialisation in Colour Imaging
% Project: Translucency Modeling and Analysis
% Instructors: Jon Y. Hardeberg
% Supervisors: Jean-Baptiste Thomas & Ivar Farup
% Description: the dipole bssrdf model.
%% ------------------------------------------------

function Rd = bssrdf(r, sigmaA, sigmaSPrime)

    sigmaTPrime = sigmaA + sigmaSPrime;
    sigmaTr= sqrt(3*sigmaA*sigmaTPrime);

    eta = 1.3;
    fdr = Fdr(eta);
    A = (1.0 + fdr)/(1.0 - fdr);
    zr = 1./sigmaTPrime; dr = sqrt(zr.^2 + r.^2);
    zv = zr*(1+((4*A)/3)); dv = sqrt(zv.^2 + r.^2)
    ;

    alphaPrime = sigmaSPrime/sigmaTPrime;
    sTrDr = sigmaTr * dr;
    sTrDv = sigmaTr * dv;

    Rd = (0.25.*inv(pi)*alphaPrime)*( ...
            ((zr.*(1+sTrDr).*exp(-sTrDr))./(dr.^3)
    ) + ...
            ((zv.*(1+sTrDv).*exp(-sTrDv))./(dv.^3)
    ));
end
```

Listing 1. R_d function represented by r

Instead of using $log(E)$ (obtained from section 4.2), the fitting was performed between R_d and $E = e^{log(E)}$. It is important to notice that before the fitting, a change on scale was performed using the values of a perfect diffuser capture in the same conditions. From this fitting, it was obtained an absorption of $\sigma_a = 9.2787 \times 10^{-12}\ mm^{-1}$ and scattering of $\sigma_s' = 3.0950\ mm^{-1}$ for the physical parameters of the sample.

Figure 11 shows the resulting fitting.

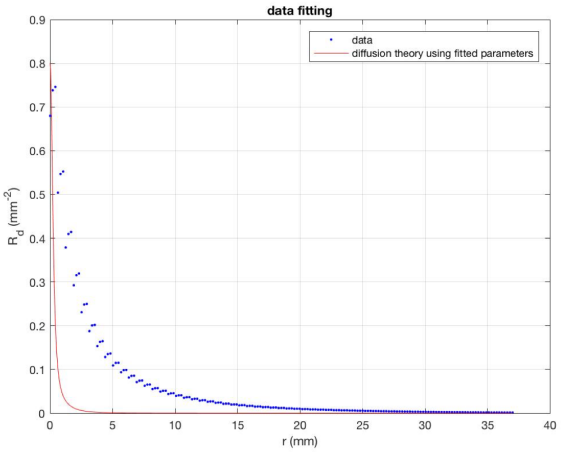

Figure 11. Fitting of R_d dipole approximation and E.

4.4 Evaluation

The evaluation performed was a robustness measurement. For this, the same procedure was followed, but choosing a different 2D area of interest (instead of choosing the right part of the sample, choosing the left). The results were an absorption of $\sigma_a = 5.7683 \times 10^{-12}\ mm^{-1}$ and scattering of $\sigma_s' = 2.8622\ mm^{-1}$, showing a confirmation of the performance of the system for different 2D diffusion areas.

5. Discussion

An analysis on the obtained results from section 4 is done. The three main focuses are: (1) HDR radiance maps, (2) data fitting and (3) evaluation.

For the HDR radiance maps, the method of Debevec and Malik [6] was used twice. First, it was to compute the HDR image and its tone mapping displayed version. The objective was to see from the image how the beam of light from the

laser arrived to the middle point in the material (in this case milk) and it diffused through the rest of the surface. However, for this to be possible the difference of the laser hitting point and its diffused light needed to be noticeable on the resulting tone map image. The first attempt was to use a linear tone mapping method, but the result was a blurred image. Later, it was analyzed the behavior of the LRD images and its exposures. It was found that the best solution was a global tone mapping operator of $log(L)$.

From the HDR tone map representation, the selection of the correct area of interest (the 2D region), was easier. The range selected was only the part where the diffusion of the light was visible (discarding the laser and the glass). This was the second time where the Debevec and Malik [6] algorithm was used. Both g and $log(E)$ functions were found from the averaged 1D slice. Normally, when trying to describe a camera response, the g function is the one needed. Nevertheless, because the objective was to fit R_d model to the data, the purpose was to use $log(E)$ to fit $log(R_d)$.

When the process of fitting the model was carried out, some drawbacks arose. First of all, it was found little amount of work related to the inverse rendering of the dipole model. The documents found only mentioned the data obtained by Jensen et al. [18] in their implementation. On the other hand, the acquisition process was analyzed carefully and it was found that the capturing of a perfect diffuser was missing, which was necessary for the scaling process of $log(E)$. However, this discovery was made almost at the end of the implementation and a re-acquisition was not possible because of time constraints. In the end, it was used the value of 0.97 (normalized) as the diffuser value, but this affected the final fitting and the scale of the absorption σ_a and scattering σ_s' resulting parameters.

Finally, the evaluation process only measured the robustness of the implementation. Nevertheless, it is possible to say that other forms of evaluation are possible too. As mentioned on section 1, different methods have been developed. However, it is important to notice that some of this methods take more time to be implemented (e.g. the Monte Carlo method can be used to evaluate the results, but its implementation and run time are much greater). Due to time constraints, here it was only mentioned this methods, but the possibility remains for future work.

In summary, an HDR image was generated from the dataset of 46 LRD images. To display the result, a global log tone map was applied. It was selected a 2D region on the image, where the diffusion of light on the surface was observed on the sample. The slices were then averaged to a 1D representation. Both g and $log(E)$ were obtained, but only $log(E)$ was fitted to the dipole model. From the fitting, it was obtained the absorption σ_a and scattering σ_s' parameters of the sample. An evaluation of the robustness of the system was performed by doing the same procedure, but selecting another 2D region of interest.

6. Conclusion and Future Work

From the previous results and analysis (section 4 and 5), it is possible to say that it was achieved a practical methodology of the known approximation method of dipole BSSRDF by using the inverse rendering method. Additionally, the work presented by Alkaoui [1] was continued and the final stage of the method was reached.

As future work, the possible improvements needed to be consider are:

1. Try to follow the complete process of inverse rendering from the start (figure 3). More than that, the model and the method should be understood completely before starting the acquisition.

2. Consider the idea of testing different samples (e.g. different types of milk - whole , skim, almond, soya, etc.). Since the proposed inverse rendering method is a fluid process, it can be applied individually to each desired sample. Then, these results can be compared to see the behavior of each sample and the samples as a unit.

3. For the final evaluation step, consider other methods. Depending on the time, methods like photo mapping and Monte Carlo can be also used to compare the results.

Acknowledgments

I would like to thank professors Jean-Baptiste Thomas and Ivar Farup, who provided the insight and expertise that greatly assisted the research. I thank Najwa Alkaoui for the acquired measurements from her Master Thesis, that were used on the research. I would also like to show my gratitude to professor Jon Hardeberg for sharing his wisdom with us during the Specialisation in Colour Imaging course.

References

[1] N. Alkaoui. Translucent material analysis and modeling. Master's thesis, University of Burgundy, France, 2017.

[2] A. Arbree, B. Walter, and K. Bala. Heterogeneous subsurface scattering using the finite element method. *IEEE Transactions on Visualization and Computer Graphics*, 17(7):956–969, July 2011. ISSN 1077-2626. doi: 10.1109/TVCG.2010.117. URL http://dx.doi.org/10.1109/TVCG.2010.117.

[3] B. Bitterli. BSSRDF Explorer: A rendering framework for the BSSRDF. Master's thesis, Swiss Federal Institute of Technology Zurich, Switzerland, 2013.

[4] C. Dachsbacher, J. Křivánek, M. Hašan, A. Arbree, B. Walter, and J. Novák. Scalable realistic rendering with many-light methods. *Comput. Graph. Forum*, 33(1):88–104, Feb. 2014. ISSN 0167-7055. doi: 10.1111/cgf.12256. URL http://dx.doi.org/10.1111/cgf.12256.

[5] P. Debevec. Rendering synthetic objects into real scenes: Bridging traditional and image-based graphics with global illumination and high dynamic range photography. In *ACM SIGGRAPH 2008 Classes*, SIGGRAPH '08, pages 32:1–32:10, New York, NY, USA, 2008. ACM. doi: 10.1145/1401132.1401175. URL http://doi.acm.org/10.1145/1401132.1401175.

[6] P. E. Debevec and J. Malik. Recovering high dynamic range radiance maps from photographs. In *Proceedings of the 24th Annual Conference on Computer Graphics and Interactive Techniques*, SIGGRAPH '97, pages 369–378, New York, NY, USA, 1997. ACM Press/Addison-Wesley Publishing Co. ISBN 0-89791-896-7. doi: 10.1145/258734.258884. URL http://dx.doi.org/10.1145/258734.258884.

[7] E. D'Eon and G. Irving. A quantized-diffusion model for rendering translucent materials. *ACM Trans. Graph.*, 30(4):56:1–56:14, July 2011. ISSN 0730-0301. doi: 10.1145/2010324.1964951. URL http://doi.acm.org/10.1145/2010324.1964951.

[8] Y. Dobashi, W. Iwasaki, A. Ono, T. Yamamoto, Y. Yue, and T. Nishita. An inverse problem approach for automatically adjusting the parameters for rendering clouds using photographs. *ACM Trans. Graph.*, 31(6):145:1–145:10, Nov. 2012. ISSN 0730-0301. doi: 10.1145/2366145.2366164. URL http://doi.acm.org/10.1145/2366145.2366164.

[9] C. Donner. *Towards Realistic Image Synthesis of Scattering Materials*. PhD thesis, University of California, San Diego, 2006.

[10] C. Donner and H. W. Jensen. Rendering translucent materials using photon diffusion. In *ACM SIGGRAPH 2008 Classes*, SIGGRAPH '08, pages 4:1–4:9, New York, NY, USA, 2008. ACM. doi: 10.1145/1401132.1401138. URL http://doi.acm.org/10.1145/1401132.1401138.

[11] C. Donner, J. Lawrence, R. Ramamoorthi, T. Hachisuka, H. W. Jensen, and S. Nayar. An empirical bssrdf model. *ACM Trans. Graph.*, 28(3):30:1–30:10, July 2009. ISSN 0730-0301. doi: 10.1145/1531326.1531336. URL http://doi.acm.org/10.1145/1531326.1531336.

[12] D. Dufresne, T. Webb, S. Birch, E. Zgraggen, and J. Hays. High Dynamic Range. http://cs.brown.edu/courses/cs129/asgn/proj5/, 2002. [Online; accessed 6-November-2017].

[13] I. Gkioulekas, S. Zhao, K. Bala, T. Zickler, and A. Levin. Inverse volume rendering with material dictionaries. *ACM Trans. Graph.*, 32(6):162:1–162:13, Nov. 2013. ISSN 0730-0301. doi: 10.1145/2508363.2508377. URL http://doi.acm.org/10.1145/2508363.2508377.

[14] P. Gkioulekas, B. Walter, E. Adelson, K. Bala, and T. Zickler. On the appearance of translucent edges. In *Proceedings of the IEEE Conference on Computer Vision and Pattern Recognition*. CVPR, 2015. URL http://vision.seas.harvard.edu/translucentedges/lipaths.pdf.

[15] R. Habel, P. H. Christensen, and W. Jarosz. Photon beam diffusion: A hybrid monte carlo method for subsurface scattering. In *Proceedings of the Eurographics Symposium on Rendering*, EGSR '13, pages 27–37, Aire-la-Ville, Switzerland, Switzerland, 2013. Eurographics Association. doi: 10.1111/cgf.12148. URL http://dx.doi.org/10.1111/cgf.12148.

[16] T. Hachisuka, W. Jarosz, G. Bouchard, P. Christensen, J. R. Frisvad, W. Jakob, H. W. Jensen, M. Kaschalk, C. Knaus, A. Selle, and B. Spencer. State of the art in photon density estimation. In *ACM SIGGRAPH 2012 Courses*, SIGGRAPH '12, pages 6:1–6:469, New York, NY, USA, 2012. ACM. ISBN 978-1-4503-1678-1. doi: 10.1145/2343483.2343489. URL http://doi.acm.org/10.1145/2343483.2343489.

[17] H. W. Jensen and J. Buhler. A rapid hierarchical rendering technique for translucent materials. *ACM Trans. Graph.*, 21(3):576–581, July 2002. ISSN 0730-0301. doi: 10.1145/566654.566619. URL http://doi.acm.org/10.1145/566654.566619.

[18] H. W. Jensen, S. R. Marschner, M. Levoy, and P. Hanrahan. A practical model for subsurface light transport. In *Proceedings of the 28th Annual Conference on Computer Graphics and Interactive Techniques*, SIGGRAPH '01, pages 511–518, New York, NY, USA, 2001. ACM. ISBN 1-58113-374-X. doi: 10.1145/383259.383319. URL http://doi.acm.org/10.1145/383259.383319.

[19] J. T. Kajiya and B. P. Von Herzen. Ray tracing volume densities. *SIGGRAPH Comput. Graph.*, 18(3):165–174, Jan. 1984. ISSN 0097-8930. doi: 10.1145/964965.808594. URL http://doi.acm.org/10.1145/964965.808594.

[20] E. P. Lafortune and Y. D. Willems. Rendering participating media with bidirectional path tracing. In *Proceedings*

of the Eurographics Workshop on Rendering Techniques '96, pages 91–100, London, UK, UK, 1996. Springer-Verlag. ISBN 3-211-82883-4. URL http://dl.acm.org/citation.cfm?id=275458.275468.

[21] H. Li, F. Pellacini, and K. E. Torrance. A hybrid monte carlo method for accurate and efficient subsurface scattering. In *Proceedings of the Sixteenth Eurographics Conference on Rendering Techniques*, EGSR '05, pages 283–290, Aire-la-Ville, Switzerland, Switzerland, 2005. Eurographics Association. ISBN 3-905673-23-1. doi: 10.2312/EGWR/EGSR05/283-290. URL http://dx.doi.org/10.2312/EGWR/EGSR05/283-290.

[22] S. R. Marschner. *Inverse Rendering for Computer Graphics*. PhD thesis, Cornell University, New York, 1992.

[23] F. E. Nicodemus, J. C. Richmond, J. J. Hsia, I. W. Ginsberg, and T. Limperis. Radiometry. chapter Geometrical Considerations and Nomenclature for Reflectance, pages 94–145. Jones and Bartlett Publishers, Inc., USA, 1992. ISBN 0-86720-294-7. URL http://dl.acm.org/citation.cfm?id=136913.136929.

[24] M. Papas, C. Regg, W. Jarosz, B. Bickel, P. Jackson, W. Matusik, S. Marschner, and M. Gross. Fabricating translucent materials using continuous pigment mixtures. *ACM Trans. Graph.*, 32(4):146:1–146:12, July 2013. ISSN 0730-0301. doi: 10.1145/2461912.2461974. URL http://doi.acm.org/10.1145/2461912.2461974.

[25] M. Pauly, T. Kollig, and A. Keller. Metropolis light transport for participating media. In *Proceedings of the Eurographics Workshop on Rendering Techniques 2000*, pages 11–22, London, UK, UK, 2000. Springer-Verlag. ISBN 3-211-83535-0. URL http://dl.acm.org/citation.cfm?id=647652.732117.

[26] J. Stam. *Multiple scattering as a diffusion process*, pages 41–50. Springer Vienna, Vienna, 1995. ISBN 978-3-7091-9430-0. doi: 10.1007/978-3-7091-9430-0_5. URL https://doi.org/10.1007/978-3-7091-9430-0_5.

[27] J. Wang, S. Zhao, X. Tong, S. Lin, Z. Lin, Y. Dong, B. Guo, and H.-Y. Shum. Modeling and rendering of heterogeneous translucent materials using the diffusion equation. *ACM Trans. Graph.*, 27(1):9:1–9:18, Mar. 2008. ISSN 0730-0301. doi: 10.1145/1330511.1330520. URL http://doi.acm.org/10.1145/1330511.1330520.

[28] D. R. Wyman, M. S. Patterson, and B. C. Wilson. Similarity relations for the interaction parameters in radiation transport. *Appl. Opt.*, 28(24):5243–5249, Dec 1989. doi: 10.1364/AO.28.005243. URL http://ao.osa.org/abstract.cfm?URI=ao-28-24-5243.

[29] S. Zhao, R. Ramamoorthi, and K. Bala. High-order similarity relations in radiative transfer. *ACM Trans. Graph.*, 33(4):104:1–104:12, July 2014. ISSN 0730-0301. doi: 10.1145/2601097.2601104. URL http://doi.acm.org/10.1145/2601097.2601104.